

Analysis of Thermodynamic Properties for Rare Earth Complexes in Ionic Liquids by Raman Spectroscopy and DFT Calculation

Masahiko Matsumiya^{1,*}, Ryo Kazama¹ and Katsuhiko Tsunashima²

¹Graduate School of Environment and Information Sciences, Yokohama National University, 79-2 Tokiwadai, Hodogaya-ku, Yokohama, 240-8501, Japan

²Department of Materials Science, Wakayama National College of Technology, 77 Noshima, Nada-cho, Gobo, Wakayama, 644-0023, Japan

Abstract: The coordination states of the divalent and trivalent rare earth complexes in ionic liquid, triethyl-pentyl-phosphonium bis(trifluoromethyl-sulfonyl) amide [P₂₂₂₅][TFSA] were investigated by Raman spectroscopy and DFT calculation. The concentration dependences of the deconvoluted Raman spectra were investigated for 0.23–0.45 mol kg⁻¹ RE(III), RE=Nd and Dy, and the mixed sample of RE(II)/RE(III)=1/3 at the molar ratio in [P₂₂₂₅][TFSA]. According to the conventional analysis, the solvation number; *n* of rare earth complexes in [P₂₂₂₅][TFSA] were determined to be *n*=4.06 for Nd(II), 5.01 for Nd(III), 4.12 for Dy(II) and 5.00 for Dy(III).

Thermodynamic properties such as $\Delta_{\text{iso}}G$, $\Delta_{\text{iso}}H$ and $\Delta_{\text{iso}}S$ for the isomerism of [TFSA] from *trans*- to *cis*-isomer in bulk and the first solvation sphere of the centered [RE³⁺] cation in [P₂₂₂₅][TFSA] were evaluated from the temperature dependence in the range of 298–398 K. $\Delta_{\text{iso}}G(\text{bulk})$, $\Delta_{\text{iso}}H(\text{bulk})$ and $T\Delta_{\text{iso}}S(\text{bulk})$ at 298 K were -1.06, 6.86, and 7.92 kJ mol⁻¹, respectively. The *trans*-[TFSA] was dominant in the enthalpy due to the positive value of $\Delta_{\text{iso}}H(\text{bulk})$ and $T\Delta_{\text{iso}}S(\text{bulk})$ was slightly larger than $\Delta_{\text{iso}}H(\text{bulk})$, so that *cis*-[TFSA] was revealed to be an entropy-controlled in [P₂₂₂₅][TFSA]. On the other hand, in the first solvation sphere of [RE³⁺] cation, $\Delta_{\text{iso}}H(\text{Nd})$ (-47.39 kJ mol⁻¹) increased to the negative value remarkably and implied that the *cis*-[TFSA] isomers were stabilized for enthalpy. $\Delta_{\text{iso}}H(\text{Nd})$ contributed to the remarkable decrease in the $\Delta_{\text{iso}}G(\text{Nd})$ and this result clearly indicated that the *cis*-[TFSA] bound to Nd³⁺ cation was preferred and the coordination state of [Dy^(III)](*cis*-TFSA)₅²⁻ was stable in [P₂₂₂₅][TFSA].

The optimized geometries and the bonding energies of [RE^(III)](*cis*-TFSA)₄²⁻ and [RE^(III)](*cis*-TFSA)₅²⁻ clusters were also investigated from DFT calculation with ADF package. The bonding energy; ΔE_{b} was calculated from $\Delta E_{\text{b}} = E_{\text{tot}}(\text{cluster}) - E_{\text{tot}}(\text{RE}^{2,3+}) - nE_{\text{tot}}([\text{TFSA}])$. $\Delta E_{\text{b}}([\text{Nd}^{(III)}](\text{cis-TFSA})_4^{2-})$, $\Delta E_{\text{b}}([\text{Nd}^{(III)}](\text{cis-TFSA})_5^{2-})$, $\Delta E_{\text{b}}([\text{Dy}^{(III)}](\text{cis-TFSA})_4^{2-})$ and $\Delta E_{\text{b}}([\text{Dy}^{(III)}](\text{cis-TFSA})_5^{2-})$ were -2241.6, -4362.3, -2135.4 and -4284.2 kJmol⁻¹, respectively. This result was revealed that [RE^(III)](*cis*-TFSA)₅²⁻ cluster formed stronger coordination bonds than [Dy^(III)](*cis*-TFSA)₄²⁻ cluster. The average atomic charges and the bond distances of these clusters were consistent with the thermodynamic properties.

Keywords: Coordination state, DFT calculation, Rare earth, Raman spectroscopy, Thermodynamic property.

1. INTRODUCTION

Rare earth (RE) elements have peculiar physicochemical properties and are indispensable for abrasives, catalysts, fluorescent materials and permanent magnets [1-4]. In particular, Nd-Fe-B permanent magnets have high ferromagnetic performance and it has been used for a variety of high-tech products, such as voice coil motors in hard disk drives, magnetic field sources for magnetic resonance imaging, driving motors for hybrid-type electric vehicles etc. [5-7]. Nd and Dy are very important RE element for Nd-Fe-B magnets because Nd is main component of Nd-Fe-B alloy and Dy protects the ferromagnetism at high temperatures. However, it is difficult to supply RE elements continuously due to uneven distribution of their resources and diplomatic reasons. Therefore, it is very important to establish a recovery process of Nd and Dy from the spent Nd-Fe-B magnets in order to

provide a steady supply of RE resources. For this purpose, our research group has already demonstrated the electrodeposition method of Nd [8-12] and Dy [13, 14] metals using room-temperature ionic liquids (RTILs), which have several distinctive properties such as low vapor pressure, incombustibility, high ionic conductivity and a wide electrochemical window [15, 16]. In particular, the RTIL composed of phosphonium cation with short alkyl chain and bis(trifluoromethyl-sulfonyl)amide anion; [TFSA] was appropriate for the electrodeposition of RE metals because of low viscosity at elevated temperatures and high thermal stability compared with other RTILs [17].

In general, it was known that the electrodeposition process was remarkably affected by the solvation structure of metal ion in ILs. It was reported that the solvation structures of various metal ions, Li [19-23], Mn [24, 25], Fe [26], Co [24, 26], Ni [24, 26], Zn [24], Nd [10, 27], Eu [28] and Dy [29] ions in [TFSA]-based ILs were evaluated by Raman spectroscopy and DFT calculation. It has also revealed that the solvation structures and the electrochemical behaviors of

*Correspondence Address to this author at the Graduate School of Environment and Information Sciences, Yokohama National University, 79-2 Tokiwadai, Hodogaya-ku, Yokohama, 240-8501, Japan; Tel/Fax: +81-45-339-3464; E-mail: mmatsumi@ynu.jp

trivalent Nd and Dy cations in order to reveal the electrodeposition mechanism in our previous study [14]. In our findings, the reduction process of trivalent Nd and Dy cations proceeded in two steps by way of divalent of Nd and Dy cations [RE(III) + e⁻ → RE(II), RE(II) + 2e⁻ → RE(0), RE=Nd and Dy]. However, there were no information about the detailed solvation conformations of Nd(II) and Dy(II) except for our recent research [29]. Therefore, we have investigated the solvation number and the isomeric characteristic of the [TFSA]⁻ ligand of RE(II) and RE(III) complexes by means of Raman spectroscopic analysis in this study. In addition, to discuss the optimum geometries of RE(II) and RE(III) complexes in more detail, we adopted the theoretical DFT calculations by Amsterdam Density Functional (ADF) program package (version 2014.01) [30-34]. The ADF package can perform a full-electron calculation for all elements including heavy atoms such as RE metals.

In this way, the methodology both experimental approach and computational analysis enables us to deeply understand the coordination states of RE(II) and RE(III) complexes in ILs. In this paper, the solvation number and the [TFSA]⁻ isomer analysis of RE(II) and RE(III) complexes in [TFSA]-based ILs were investigated from the band intensity analysis and thermodynamic analysis by Raman spectroscopy. Moreover, the optimum geometries and the bonding energies of RE(II) and RE(III) complexes were also examined using ADF package in order to understand the stability of their coordination states.

2. EXPERIMENTAL

2.1. Preparation

The IL of triethyl-*n*-pentyl-phosphonium bis (trifluoromethyl-sulfonyl) amide; [P₂₂₂₅][TFSA] used in this study was synthesized by a metathesis reaction between [P₂₂₂₅]Br (Nippon Chemical Industrial Co., Ltd., >99.5 %) and Li[TFSA] (Kanto Chemical Co., Inc., 99.7 %) as described in the previous reference [35]. The absence of bromide anion in IL was confirmed by titration with AgNO₃ after repeated washing of IL with distilled water. The obtained [P₂₂₂₅][TFSA] was dried under high vacuum < -0.1 MPa at 393 K for more than 48 h. Nd(TFSA)₃ and Dy(TFSA)₃ salts were synthesized by a neutralization reaction between Nd₂O₃ (Wako Pure Chemical Industries Ltd, 99.9%) and Dy₂O₃ (Kanto Chemical Co., Inc., 99.95 %) and 1,1,1-Trifluoro-*N*-[(trifluoromethyl)sulfonyl]methanesulfonamide (HTFSA, Kanto Chemical Co., Inc., 99.8 %)

in an aqueous solution, respectively. The unreacted acid and water components in the resulting products were removed by evaporation at 393 K. Nd(TFSA)₃ and Dy(TFSA)₃ salts were dried in vacuo < -0.1 MPa at 393 K for 24 h.

2.2. Raman Spectroscopy

At first, four kinds of Nd(III) and Dy(III) solutions were prepared by dissolving the appropriate amounts of Nd(TFSA)₃ and Dy(TFSA)₃ salts into [P₂₂₂₅][TFSA] at the concentration of 0.23, 0.30, 0.38 and 0.45 mol kg⁻¹, respectively. Raman spectra (NRS-4100, JUSCO Corp.) were measured at 298 K and 373 K using 532 nm laser for Nd, and 785 nm laser for Dy. The appropriate gratings for Raman spectrum were 1800 mm⁻¹ for Nd, and 1200 mm⁻¹ for Dy. These conditions were adopted in order to prevent the effect of fluorescence of RE ions based on the recent our investigations [26, 27]. In order to analyze the solvation number of RE(II), RE=Nd and Dy in [P₂₂₂₅][TFSA], according to the previous study [14] the mixed samples of RE(II)/RE(III) complexes for Raman spectroscopy were prepared by the controlled potential electrolysis (CPE) method based on the electrochemically reduction reaction. The induced overpotential on the working electrode was maintained at -2.5 V during CPE, because the apparent potential of RE(II)/RE(III) was determined from the following equation in the previous EMF study [14].

$$E_{\text{Nd(II)/Nd(III)}} = -2.3628 + 0.0326 \ln([\text{Nd(III)}]/[\text{Nd(II)}]) \quad (1)$$

$$E_{\text{Dy(II)/Dy(III)}} = -2.4463 + 0.0324 \ln([\text{Dy(III)}]/[\text{Dy(II)}]) \quad (2)$$

The number of electron transferred at -2.36V and -2.45V was confirmed to be one by the slope of above equations. Pt disk electrode with surface area: 2.0 × 10⁻⁵ m² was employed as a working electrode. Pt wire with 0.5 mm inside diameter was used as a quasi-reference electrode (QRE). A counter electrode of Pt wire with 0.5mm inside diameter was isolated from the electrolyte with Vycor glass filter in order to prevent the decomposition of the bulk sample. After CPE, the molar ratio of RE(II)/RE(III) in IL was confirmed to be 1:3 for all samples.

The sample solutions for analysis of [TFSA]⁻ isomer were prepared by dissolving RE(TFSA)₃ into [P₂₂₂₅][TFSA]. The molar fractions of RE(III) in the sample solutions, *x*_{RE}, were 0.000, 0.033, 0.055 and 0.075. Raman spectra were measured at various temperatures, 298, 323, 348, 373 and 398 K. All of

Raman spectra were accumulated 512 times in order to keep a sufficiently high S/N ratio. The overlapping Raman bands were deconvoluted into single component with a pseudo-Voigt function.

2.3. Calculation Methods

DFT calculations of ILs were carried out using the Gaussian 09 program package [36]. The geometry optimization and the frequency calculations of $[P_{2225}]^+$ and $[TFSA]^-$ were calculated with the basis set of B3LYP/6-31G(d,p) [37-41] and B3LYP/6-31+G(d), respectively. The B3LYP of hybrid functional, which include a mixture of Hartree-Fock exchange with DFT exchange-correlation, is Becke's three-parameter hybrid method (B3) [42] with the non-local correlation provided by Lee, Yang, and Parr (LYP) [43]. The 6-31G with diffuse and polarization functions was applied to the basis set.

On the other hand, the clusters of $[RE^{(III)}(TFSA)_4]^{2-}$ and $[RE^{(III)}(TFSA)_5]^{2-}$ complexes were calculated by ADF program package [34] using BP (Becke88-Perdew86 functional [44-47]) /TZP for Pr, Nd and Dy, and BP/DZP for light elements. The ADF adopts the Slater-type orbital (STO) which describes atomic orbitals more exactly than Gauss-type orbital (GTO). Moreover, all electron and frozen-core basis sets are available for all elements including lanthanides and actinides because the ADF adopts the Zeroth-Order Regular Approximation (ZORA) method [48-50]. The

frozen-core approximation can be used to considerably reduce the computation time for systems with heavy nuclei.

3. RESULTS AND DISCUSSION

3.1. Analysis of the Solvation Number

The concentration dependences of the deconvoluted Raman spectra in the frequency range 720–780 cm^{-1} for 0.23–0.45 mol kg^{-1} pure Nd(III) sample in $[P_{2225}][TFSA]$ and the mixed sample of Nd(II)/Nd(III)=1/3 at the molar ratio in $[P_{2225}][TFSA]$ were shown in Figures 1a and 1b, respectively. The Raman spectra in this range were separated into two components at approximately 740 cm^{-1} and 751 cm^{-1} . It is known that these Raman bands are ascribed to the combination of the stretching vibration $\nu_s(\text{SNS})$ and the bending vibration $\delta_s(\text{CF}_3)$ of the $[TFSA]^-$ anion [51, 52]. These two bands at 740 cm^{-1} and 751 cm^{-1} are caused by the free $[TFSA]^-$ anion and the $[TFSA]^-$ anion bound to Nd^{3+} ion, respectively. As can be seen from Figure 1, a new band at 751 cm^{-1} was observed as a shoulder of the band at 740 cm^{-1} . This new band intensified with increasing the concentration of Nd(III) in IL.

The solvation number of Nd(II) in $[P_{2225}][TFSA]$ was evaluated using the similar analysis method suggested by Umebayashi *et al.* [20, 21]. The intensity of the deconvoluted Raman band of free $[TFSA]^-$ anions in the bulk IL was represented as $I_f = J_f c_f$, where J_f and c_f

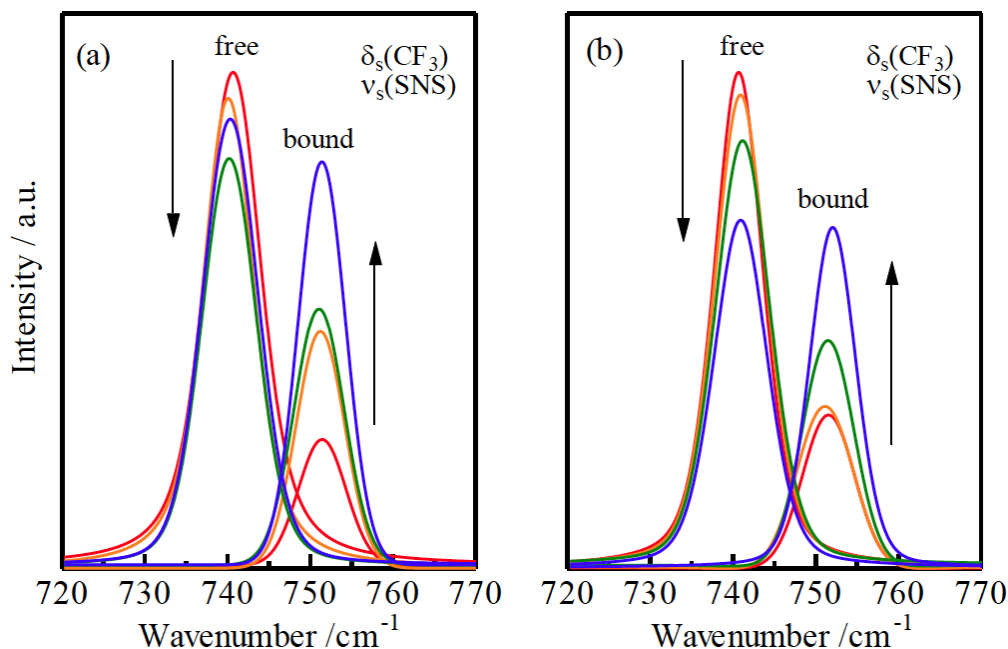


Figure 1: Raman spectra of $[P_{2225}][TFSA]$ containing 0.23, 0.30, 0.38 and 0.45 mol kg^{-1} (a) Nd(III) samples and (b) Nd(II)/Nd(III) mixed samples at 298 K.

were the molar Raman scattering coefficient and the concentration of free [TFSA]⁻ anions in the bulk, respectively. The c_f value was represented as $c_f = c_T - c_b = c_T - nc_M$, where c_T , c_b , c_M , and n expressed for the concentration of total [TFSA]⁻ anions, that of bound [TFSA]⁻ anions (solvated to the metal ion), that of metal ion, and the solvation number of the metal ion, respectively. By inserting $c_f = c_T - c_b = c_T - nc_M$ into $I_f = J_f c_f$, the following equation was obtained:

$$I_f / c_M = J_f (c_T / c_M - n) \quad (3)$$

The plot of I_f / c_M against c_T / c_M leads a straight line if the solvation number of the Nd cation in [P₂₂₂₅][TFSA] is constant. Thus, the value of n is obtained using $n = -\beta/\alpha$ from a slope of $\alpha = J_f$ and an intercept of $\beta = -J_f n$. The plots of I_f / c_M against c_T / c_M for [P₂₂₂₅][TFSA] ILs containing 0.23–0.45 mol kg⁻¹ Nd(III) and Nd(II)/Nd(III) mixed samples, were represented in Figures 2a and 2b, respectively. As shown in these plots, the strong linear relationship indicated that the number of the [TFSA]⁻ anion solvated to the Nd(II) and Nd(III) was maintained unchanged under the examined experimental conditions. Hence, the estimated n values of Nd(III) and Nd(II)/Nd(III) mixed sample were evaluated as $n_{\text{Nd(III)}} = 5.01$ and $n_{\text{Nd(II)/Nd(III)}} = 4.69$, respectively. This result suggested that the centered [Nd³⁺] cation in [P₂₂₂₅][TFSA] was solvated by five [TFSA]⁻ anions and the complexation of [Nd(TFSA)₅]²⁻ cluster existed in this system. In addition, considering that the molar ratio of mixed samples, Nd(II)/Nd(III) is 1/3, the result of $n_{\text{Nd(II)/Nd(III)}} = 4.69$ allowed us to conclude

that the solvation number of Nd(II) in [P₂₂₂₅][TFSA] was $n_{\text{Nd(II)}} = 4.06$. In the case of Dy, the result of $n_{\text{Dy(II)/Dy(III)}} = 4.78$ indicated that the solvation number of Dy(II) in [P₂₂₂₅][TFSA] was $n_{\text{Dy(II)}} = 4.12$. Therefore, the centered RE²⁺ cation was found to be existed as the complex state of [RE(TFSA)₄]²⁻ cluster in [P₂₂₂₅][TFSA]. It was found that the solvation number of [TFSA]⁻ anion on the centered RE²⁺ cation was smaller than that on the centered RE³⁺ cation. This decrease in the solvation number would be due to the difference in ionic valence of the centered cation metals. This result was also consistent with the previous result that the diffusion coefficient [14] of Dy(II) was larger than that of Dy(III) in [P₂₂₂₅][TFSA]. Thus, the definite difference of the diffusion coefficient between Dy(II) and Dy(III) clusters would be due to the difference of electrostatic interaction between the centered metal ion and the surrounding [TFSA]⁻ anion by the solvation structure in [TFSA]-based ILs.

3.2. Thermodynamic Stability for [TFSA]⁻ Isomerism

The temperature dependence of Raman spectra for Nd(III) in [P₂₂₂₅][TFSA] ($x_{\text{Nd}} = 0.000, 0.033, 0.055$ and 0.075) was measured in order to evaluate the thermodynamic stability for [TFSA]⁻ isomerism. Temperature dependences of the deconvoluted Raman spectra for (a) neat [P₂₂₂₅][TFSA], (b) Nd(III) in [P₂₂₂₅][TFSA] ($x_{\text{Nd(III)}} = 0.033$) and (c) Dy(III) in [P₂₂₂₅][TFSA] ($x_{\text{Dy(III)}} = 0.033$) in the frequency range of 370–440 cm⁻¹ were shown in Figures 3a, 3b and 3c, respectively. These two peaks appeared in Figure 3

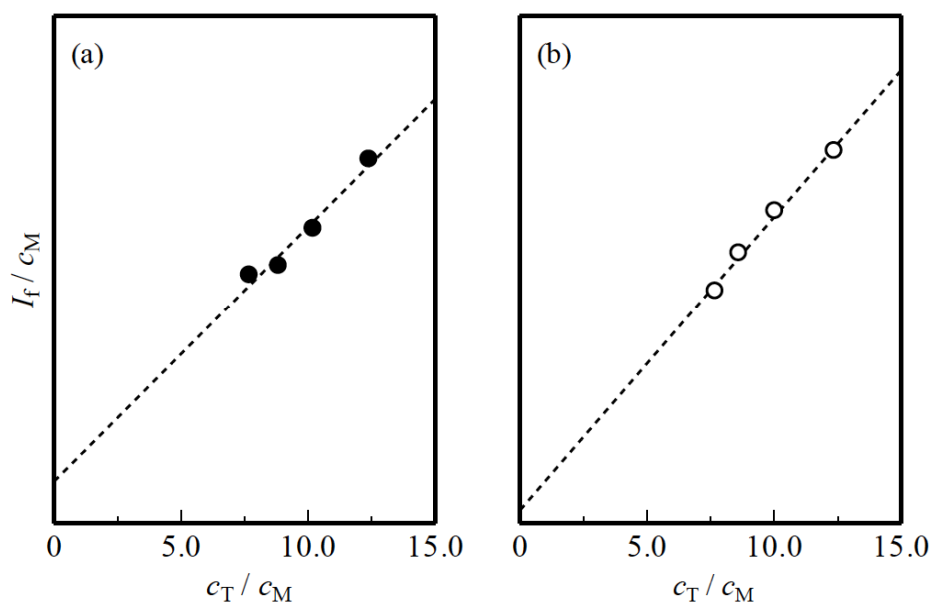


Figure 2: Plot of I_f / c_M against c_T / c_M for [P₂₂₂₅][TFSA] containing 0.23–0.45 mol kg⁻¹ (a) Nd(III) samples and (b) Nd(II)/Nd(III) mixed samples at 298 K.

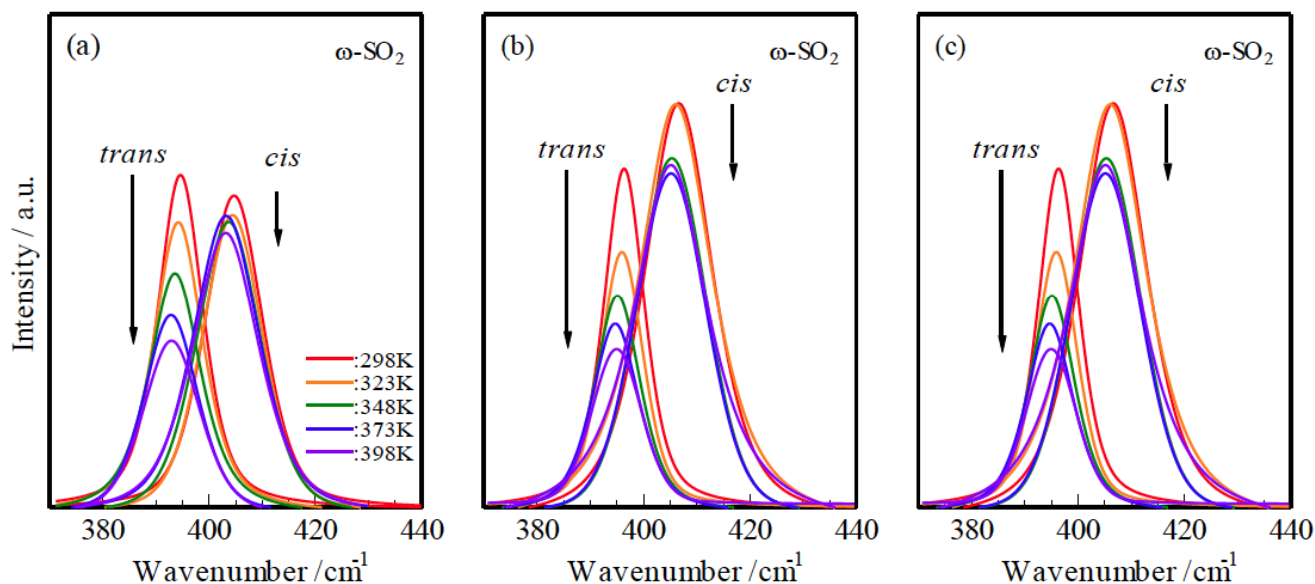


Figure 3: Temperature dependence of deconvoluted Raman spectrum of (a) neat $[P_{2225}][TFSA]$, (b) Nd(III) in $[P_{2225}][TFSA]$ ($X_{Nd(III)}=0.033$), (c) Dy(III) in $[P_{2225}][TFSA]$ ($X_{Dy(III)}=0.033$) in the frequency range of 370-440 cm^{-1} .

were suitable for analysis of the $[TFSA]^-$ isomer because there was no overlapping with Raman bands from the $[P_{2225}]^+$, as represented in Figure 4. These theoretical spectra for the optimized geometries of $[P_{2225}]^+$ cation, $trans$ - $[TFSA]^-$ and cis - $[TFSA]^-$ were calculated by DFT method at the B3LYP/6-31G(d,p) and 6-31+G(d) levels. In the range of 370-440 cm^{-1} , there were no theoretical bands in $[P_{2225}]^+$ spectrum. The bands of $trans$ - $[TFSA]^-$ and cis - $[TFSA]^-$ were assigned at 370 cm^{-1} and 380 cm^{-1} , respectively. Therefore, Raman bands of 396 cm^{-1} and 403 cm^{-1} shown in Figure 3 were corresponding to the $trans$ - $[TFSA]^-$ and cis - $[TFSA]^-$ isomers, respectively. As for the temperature dependence of neat $[P_{2225}][TFSA]$ in Figure 3a, the decreasing degree of the Raman intensity of $trans$ - $[TFSA]^-$ was larger than that of cis - $[TFSA]^-$. This result revealed that the $trans$ - $[TFSA]^-$ isomers was enthalpically stable compared to cis - $[TFSA]^-$ isomers. With regard to the Raman band of RE(III) in $[P_{2225}][TFSA]$ at $x_{RE(III)} = 0.033$, when RE(III) existed in IL, the peak area of the cis -isomers increased clearly in comparison with the band of neat $[P_{2225}][TFSA]$. This result indicated that the $[TFSA]^-$ anion solvated in RE(III) would be coordinated as the cis -isomers anion dominantly. That is to say, when $[TFSA]^-$ bound to the RE(III) in $[P_{2225}][TFSA]$, the cis - $[TFSA]^-$ isomers was more stable than the $trans$ - $[TFSA]^-$ isomers.

In order to perform a quantitative evaluation based on thermodynamics about $[TFSA]^-$ isomers, the apparent thermodynamic quantities; $\Delta_{iso}G$, $\Delta_{iso}H$ and

$T\Delta_{iso}S$ were determined from van't Hoff plots analysis [20]. The parameters of $\Delta_{iso}G$, $\Delta_{iso}H$ and $T\Delta_{iso}S$ from the $trans$ - $[TFSA]^-$ to cis - $[TFSA]^-$ as a function x_{RE} can be defined as follows. As the first step, the apparent equilibrium constant, K_{iso} for the $[TFSA]^-$ conformational isomerism from the $trans$ - $[TFSA]^-$ to cis - $[TFSA]^-$ as a function x_{RE} was defined as $K_{iso} = c_{cis}/c_{trans}$. Using this equilibrium constant, K_{iso} , $\Delta_{iso}G$ was represented as follows.

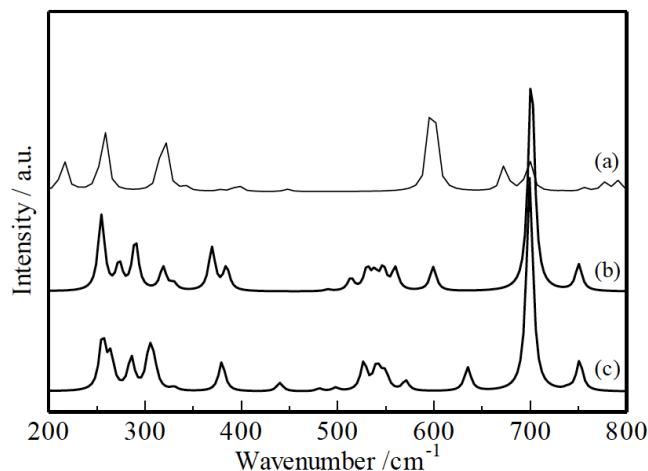


Figure 4: Theoretical Raman spectra for the optimized geometries of (a) $[P_{2225}]^+$, (b) $trans$ - $[TFSA]^-$, and (c) cis - $[TFSA]^-$ evaluated from DFT calculations.

$$\Delta_{iso}G = -RT \ln K_{iso} = -RT \ln (c_{cis}/c_{trans}) \quad (4)$$

Where R and T were a gas constant and an absolute temperature, respectively. In addition, $\Delta_{iso}G$ can be expressed as $\Delta_{iso}G = \Delta_{iso}H - T\Delta_{iso}S$ and the

Raman intensity; I is $I=Jc$. When these two equations were substituted for $\Delta_{\text{iso}}G = -RT \ln(c_{\text{cis}}/c_{\text{trans}})$, the following van't Hoff equation [20] was obtained.

$$-R \ln(I_{\text{cis}}/I_{\text{trans}}) = \Delta_{\text{iso}}H/T - \Delta_{\text{iso}}S - R \ln(J_{\text{cis}}/J_{\text{trans}}) \quad (5)$$

Where I_{cis} and I_{trans} are the Raman intensity of *cis*-[TFSA] and *trans*-[TFSA], respectively. J_{cis} and J_{trans} stand for the Raman scattering coefficients for the *cis*-[TFSA] and *trans*-[TFSA] isomers. Van't Hoff plot derived from the ratio of Raman band intensity for *cis*-[TFSA] and *trans*-[TFSA] isomers at 396 cm^{-1} and 403 cm^{-1} was shown in Figure 5. The similar measurements were performed for the samples varied in $x_{\text{RE(III)}}$ ($x_{\text{RE(III)}}=0.000, 0.033, 0.055, 0.075$) and the corresponding plots were displayed in Figure 5. The van't Hoff plot showed a good linear relation in all $x_{\text{RE(III)}}$ concentrations and the concentration dependence was confirmed in the slopes clearly. This suggested that the slopes, in other words, a value of $\Delta_{\text{iso}}H$ was able to evaluate as a function of $x_{\text{RE(III)}}$ with high accuracy. In addition, it was found that the slope of the plots ($=\Delta_{\text{iso}}H$) tended to decrease with increasing the concentration of RE(III). This result revealed that *cis*-[TFSA] was thermodynamically more stable than *trans*-[TFSA] in the system for high concentration of RE(III) and the *cis*-[TFSA] anions predominately coordinated with the centered RE^{3+} cation.

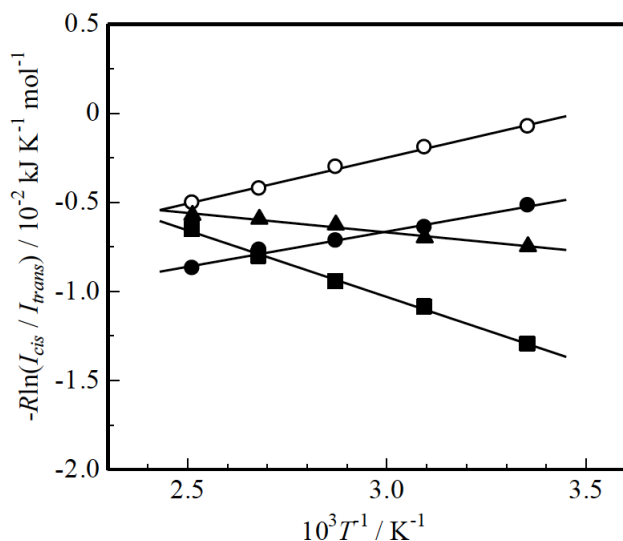


Figure 5: Van't Hoff plot for the [TFSA] isomerism in $[\text{P}_{2225}][\text{TFSA}]$ containing $\text{Nd}(\text{TFSA})_3$, (a) $x_{\text{Nd(III)}}=0.000$, (b) $x_{\text{Nd(III)}}=0.033$, (c) $x_{\text{Nd(III)}}=0.055$ and (d) $x_{\text{Nd(III)}}=0.075$.

Then, the value of $\Delta_{\text{iso}}S$ was also evaluated from the intercept of the van't Hoff plot (Figure 5) based on Eq. (5). It is necessary to consider the $J_{\text{cis}}/J_{\text{trans}}$ ratio and this value was estimated by means of the relationship of $I_{\text{cis}} = -(J_{\text{cis}}/J_{\text{trans}})I_{\text{trans}} + J_{\text{cis}}c_{\text{T}}$ [20]. From

the slope of the plots of I_{trans} against I_{cis} , it was experimentally determined that the value of $J_{\text{cis}}/J_{\text{trans}}$ ratio was 0.68. In order to confirm the reliability of this value (0.68), the theoretical calculation for the value of $J_{\text{cis}}/J_{\text{trans}}$ ratio using DFT method was carried out. The theoretical value of $J_{\text{cis}}/J_{\text{trans}}$ ratio estimated by B3LYP/6-31+G(d) level method was 0.69. Thus, an experimental value was in good accordance with a theoretical value with high accuracy, so that we applied this value to evaluate the entropy term; $\Delta_{\text{iso}}S$. Then, from the obtained value of $\Delta_{\text{iso}}H$ and $\Delta_{\text{iso}}S$, $\Delta_{\text{iso}}G (= \Delta_{\text{iso}}H - T\Delta_{\text{iso}}S)$ at 298 K were estimated as described above. All obtained thermodynamic quantities; $\Delta_{\text{iso}}G$, $\Delta_{\text{iso}}H$ and $T\Delta_{\text{iso}}S$ were plotted against the x_{RE} as shown in Figure 6. It was suggested that apparent thermodynamic quantities; $\Delta_{\text{iso}}X$ ($X=G, H$ and S) existed as a function of $x_{\text{RE(III)}}$ because the linearity was very good for all plots of thermodynamic quantities. These apparent thermodynamic quantities indicated that it was sum of those which was based on free [TFSA] anions in bulk [$\Delta_{\text{iso}}X(\text{bulk})$] and those which derived from the bonded [TFSA] anions in the first solvation sphere of the centered RE^{3+} cation [$\Delta_{\text{iso}}X(\text{RE})$]. That is to say, the apparent thermodynamic quantities; $\Delta_{\text{iso}}X$ ($X=G, H$ and S) were expressed as the following equation [20].

$$\Delta_{\text{iso}}X = nx_{\text{Dy(III)}}\Delta_{\text{iso}}X(\text{RE}) + (1-nx_{\text{Dy(III)}})\Delta_{\text{iso}}X(\text{bulk}) \quad (6)$$

Where n stands for the solvation number of RE(III), $n=5.0$. Therefore, from the relationship of Eq. (6), the values of $\Delta_{\text{iso}}X$ at $x_{\text{RE(III)}}=0$ and 0.33 are $\Delta_{\text{iso}}X(\text{bulk})$ and $\Delta_{\text{iso}}X(\text{RE})$, respectively, as shown with the broken lines in Figure 6. Thermodynamic quantities for [TFSA] of the bulk and the first solvation sphere of RE cation were listed in Table 1. As for the discussion of the bulk condition, the obtained values of $\Delta_{\text{iso}}G$ (bulk), $\Delta_{\text{iso}}H$ (bulk), and $T\Delta_{\text{iso}}S$ (bulk) at 298 K were -1.06, 6.86, and 7.92 kJ mol^{-1} , respectively. The *trans*-[TFSA] was dominant in the enthalpy due to the positive value of $\Delta_{\text{iso}}H(\text{bulk})$ (6.86 kJ mol^{-1}). $T\Delta_{\text{iso}}S(\text{bulk})$ (7.92 kJ mol^{-1}) was a positive value and slightly larger than the value of $\Delta_{\text{iso}}H$ (bulk), so that *cis*-[TFSA] was revealed to be an entropy-controlled in $[\text{P}_{2225}][\text{TFSA}]$. As a result, about the value of $\Delta_{\text{iso}}G(\text{bulk})$, it was suggested that *trans*-[TFSA] and *cis*-[TFSA] almost existed in equilibrium in neat $[\text{P}_{2225}][\text{TFSA}]$ because there were almost no differences of the Gibbs free energies (-1.06 kJ mol^{-1}) between the *trans*-isomers and the *cis*-isomers. On the other hand, in the first solvation sphere of Nd^{3+} , the value of $\Delta_{\text{iso}}H(\text{Nd})$ (-47.39 kJ mol^{-1}) increased to the negative value remarkably and implied that the *cis*-[TFSA] isomers were stabilized for

enthalpy. This value of $\Delta_{\text{iso}}H(\text{Nd})$ contributed to the remarkable decrease in the value of $\Delta_{\text{iso}}G(\text{Nd})$ which greatly changed into the negative direction ($-13.23 \text{ kJ mol}^{-1}$) compared with the $\Delta_{\text{iso}}G(\text{Nd})$. This result clearly showed that the *cis*-[TFSA] bound to the Nd^{3+} cation was preferred and the coordination state of $[\text{Nd}^{\text{III}}(\text{cis-TFSA})_5]^{2-}$ was stable in $[\text{P}_{2225}][\text{TFSA}]$. This stabilization of the *cis*-[TFSA] bound to the centered Nd^{3+} cation would be resulted from a charge-dipole interaction between the Nd^{3+} cation and *cis*-[TFSA] anion. The dipole moment of *trans*-[TFSA] and *cis*-[TFSA] estimated from DFT calculations at B3LYP/6-31+G(d) were 0.29 and 4.07, respectively. It was supposed that *cis*-[TFSA] isomer form a relatively large electric charge-dipole interaction to dysprosium ion, and form a more stable solvation structure, because the dipole moment of *cis*-[TFSA] was larger than that of *trans*-[TFSA]

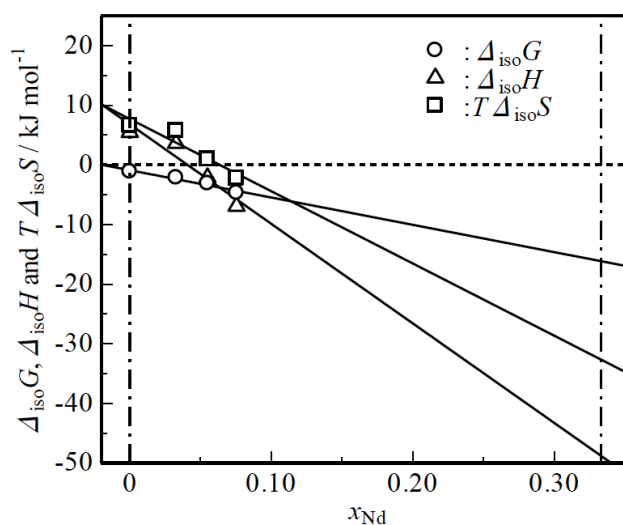


Figure 6: Apparent thermodynamic properties for the conformational isomerism of [TFSA] from the *trans*- to *cis*-isomer as a function of x_{Nd} at 298 K.

3.3. Geometries Analysis of $[\text{RE}^{\text{III}}(\text{cis-TFSA})_4]^{2-}$ and $[\text{RE}^{\text{III}}(\text{cis-TFSA})_5]^{2-}$ Clusters

From a series of results of 3.2 and 3.3 sections, the solvation numbers of RE(II) and RE(III) in $[\text{P}_{2225}][\text{TFSA}]$ were 4.0 and 5.0, respectively, and the *cis*-[TFSA]

anions predominately coordinated with RE^{3+} in the first solvation sphere of RE cation. Therefore, we applied for two clusters, $[\text{RE}^{\text{III}}(\text{cis-TFSA})_4]^{2-}$ and $[\text{RE}^{\text{III}}(\text{cis-TFSA})_5]^{2-}$ for ADF calculations in order to analysis the optimum geometries and the bonding energies for these clusters in detail. The scalar relativistic zero orders regular approximation (ZORA) method as one of the relativistic effect [48-50] was applied for the calculation of two clusters because these clusters included in a heavy RE atom. In addition, the frozen-core approximation was also introduced for relatively small calculation costs. The optimized geometries of $[\text{RE}^{\text{III}}(\text{cis-TFSA})_4]^{2-}$ and $[\text{RE}^{\text{III}}(\text{cis-TFSA})_5]^{2-}$ clusters were evaluated at BP/TZP level for RE and DZP level for other elements. In both of clusters, the oxygen atoms (O') which bound to RE cation turned out to be equally distributed in the space. The results indicated that the ligands were positioned where the repulsion energy between each ligand was minimized, because the f-orbital atoms such as lanthanides did not have a remarkable stereochemical influence for their ligands.

As for the $[\text{RE}^{\text{III}}(\text{cis-TFSA})_4]^{2-}$ complex, four [TFSA] anions behaved as a bidentate ligand by two oxygen atoms to RE^{2+} and formed the complex structure that the coordination number was 8. In some research about the metal complexes; $[\text{M}(\text{TFSA})_3]^-$ [24,26], (M=Fe, Co, Ni and Zn), some reports were indicated that the [TFSA] anions acted as a bidentate ligand and this result was consistent with these references. On the other hand, about $[\text{RE}^{\text{III}}(\text{cis-TFSA})_5]^{2-}$ complex, three [TFSA] anions were positioned as the bidentate ligands and the other two [TFSA] anions behaved as the monodentate ligands. As a result, the coordination number of $[\text{RE}^{\text{III}}(\text{cis-TFSA})_5]^{2-}$ was also maintained at 8, and which was good accordance with a result of $[\text{RE}^{\text{III}}(\text{cis-TFSA})_4]^{2-}$. In general, it was reported that the coordination number of the lanthanide aqua-complex; $[\text{Ln}(\text{OH}_2)_n]^{3+}$ was from 8 to 9. Besides T. Yaita *et al.* [53] revealed that the coordination numbers of dysprosium in aqueous nitrate and chloride solutions were assigned from 8 to 9 by EXAFS analysis. As a result, our results were consistent with the above reports.

Table 1: Thermodynamic Properties for the Isomerism of [TFSA] from the *trans*- to *cis*-isomer in Bulk and the First Solvation Sphere of Nd^{3+} and Dy^{3+} in $[\text{P}_{2225}][\text{TFSA}]$ at 298 K

Thermodynamic properties	bulk	Nd^{3+} first solvation sphere	Dy^{3+} first solvation sphere
$\Delta_{\text{iso}}G / \text{kJ mol}^{-1}$	-1.06	-13.23	-15.56
$\Delta_{\text{iso}}H / \text{kJ mol}^{-1}$	6.86	-47.39	-49.22
$T\Delta_{\text{iso}}S / \text{kJ mol}^{-1}$	7.92	-34.16	-33.66

Total bonding energy; E_{tot} of Nd(II), Nd(III), Dy(II) and Dy(III) clusters were -33246.1, -41364.7, -32754.4 and -40629.9 kJmol⁻¹, respectively. The bonding energy between the center Nd cation and [TFSA]⁻ ligands; ΔE_b was calculated according to $\Delta E_b = E_{\text{tot}}(\text{cluster}) - E_{\text{tot}}(\text{RE}^{2,3+}) - nE_{\text{tot}}([\text{TFSA}]^-)$, where n was solvation number of RE²⁺ and RE³⁺. The values thus calculated were -2241.6, -4362.3, -2135.4 and -4284.2 kJmol⁻¹ for [Nd^(II)(*cis*-TFSA)₄]²⁻, [Nd^(III)(*cis*-TFSA)₅]²⁻, [Dy^(II)(*cis*-TFSA)₄]²⁻ and [Dy^(III)(*cis*-TFSA)₅]²⁻ clusters, respectively. It was revealed that there were

approximately two times differences in each bonding energy. Therefore, it was found that [RE^(III)(*cis*-TFSA)₅]²⁻ cluster had stronger coordination bonds than [RE^(II)(*cis*-TFSA)₄]²⁻ cluster. The result of average atomic charge for each cluster was also tabulated in Table 2. This result indicated that the centered RE³⁺ cation strongly attracted with [TFSA]⁻ ligands in comparison with RE²⁺ cation because RE³⁺ cation has a high electric charge and a small ionic radius. The average atomic charges of RE cation and O' atoms for [RE^(III)(*cis*-TFSA)₅]²⁻ cluster were larger than those for

Table 2: Average Atomic Charge, Bond Length, Bond Angle, Dihedral Angle and Dipole Moment for the Optimized Geometries of [RE^(II)(*cis*-TFSA)₄]²⁻ and [RE^(III)(*cis*-TFSA)₅]²⁻ (RE=Nd and Dy) Clusters

Clusters	[Nd ^(II) (<i>cis</i> -TFSA) ₄] ²⁻	[Nd ^(III) (<i>cis</i> -TFSA) ₅] ²⁻	[Dy ^(II) (<i>cis</i> -TFSA) ₄] ²⁻	[Dy ^(III) (<i>cis</i> -TFSA) ₅] ²⁻
Atomic charge, q / e				
RE ⁿ⁺	2.042	2.473	2.077	2.545
O	-0.706	-0.716	-0.721	-0.737
O'	-0.904	-0.936	-0.932	-0.953
N	-0.962	-0.793	-0.986	-0.815
S	1.974	1.816	1.999	1.833
C	0.602	0.523	0.635	0.574
F	-0.286	-0.264	-0.303	-0.288
Bond distance, $r / \text{\AA}$				
RE ⁿ⁺ -O'	2.594	2.482	2.556	2.430
N-S	1.682	1.642	1.606	1.600
S-O	1.478	1.478	1.455	1.452
S-O'	1.482	1.491	1.477	1.488
S-C	1.912	1.912	1.891	1.890
C-F	1.371	1.382	1.353	1.351
Bond angle, $\theta / \text{deg.}$				
RE ⁿ⁺ -O'-S	142.3	146.3	145.2	147.6
O-RE ⁿ⁺ -O'	66.9	68.2	67.7	69.5
S-N-S	124.2	125.9	126.2	127.0
N-S-O	111.7	111.6	112.9	112.8
N-S-C	102.4	102.3	103.6	103.5
O-S-C	102.8	101.8	103.1	103.5
O-S-O'	117.6	116.4	118.7	118.6
S-C-F	109.4	112.6	110.5	110.2
F-C-F	107.2	109.3	108.5	108.7
Dihedral angle, $\phi / \text{deg.}$				
S-N-S-C	251.6	246.2	255.9	248.9
S-N-S-C	112.4	103.2	114.6	102.8
Dipole moment, μ / D				
	32.6	36.8	32.4	36.0

[RE^(III)(*cis*-TFSA)₄]²⁻ cluster, so that the result indicated that [RE^(III)(*cis*-TFSA)₅]²⁻ cluster had stronger coordination bonds than [RE^(III)(*cis*-TFSA)₄]²⁻ cluster. In addition, the average bond distance of RE³⁺-O' of RE(III)-cluster was shorter than RE²⁺-O' of RE(II)-cluster by 0.112Å (Nd) and 0.126Å (Dy) as listed in Table 5. The dipole moment of [RE^(III)(*cis*-TFSA)₅]²⁻ cluster were larger than those for [RE^(III)(*cis*-TFSA)₄]²⁻. A series of structural results related with clusters allowed us to conclude that [RE^(III)(*cis*-TFSA)₅]²⁻ cluster existed as more stable coordination state than [RE^(III)(*cis*-TFSA)₄]²⁻ cluster in [P₂₂₂₅][TFSA].

4. CONCLUSION

The solvation structures of the divalent and trivalent dysprosium complexes in [P₂₂₂₅][TFSA] were investigated by Raman spectroscopic analysis and DFT calculations. From the analysis of Raman intensity range of 740-751 cm⁻¹ for RE(II)/RE(III), (RE=Nd and Dy) mixed sample, the number of [TFSA]⁻ anions solvated to RE²⁺ was evaluated to be about 4, therefore, RE²⁺ cation existed as the state of [RE(TFSA)₄]²⁻ in [P₂₂₂₅][TFSA]. According to the conventional analysis, the solvation number of RE(III) in [P₂₂₂₅][TFSA] were determined to be 5.00.

Moreover, the thermodynamic stability for [TFSA]⁻ isomerism was evaluated from the van't Hoff plots from the temperature dependence of the Raman spectra. The thermodynamic properties such as $\Delta_{\text{iso}}G$, $\Delta_{\text{iso}}H$ and $\Delta_{\text{iso}}S$ for the isomerism of [TFSA]⁻ from *trans*- to *cis*- isomer in bulk and the first solvation sphere of the centered Nd³⁺ cation in [P₂₂₂₅][TFSA] were calculated in the range of 298-398 K. As for the bulk condition, $\Delta_{\text{iso}}G(\text{bulk})$, $\Delta_{\text{iso}}H(\text{bulk})$ and $T\Delta_{\text{iso}}S(\text{bulk})$ at 298 K were estimated to be -1.06, 6.86, and 7.92 kJ mol⁻¹, respectively. These results indicated that the *trans*-[TFSA]⁻ was dominant in the enthalpy and $T\Delta_{\text{iso}}S$ (bulk) was slightly larger than $\Delta_{\text{iso}}H(\text{bulk})$, so that *cis*-[TFSA]⁻ was determined to be an entropy-controlled in [P₂₂₂₅][TFSA]. On the other hand, in the first solvation sphere of Nd³⁺ cation, $\Delta_{\text{iso}}H(\text{Nd})$ increased to the negative value (-47.39 kJ mol⁻¹) remarkably and revealed that the *cis*-[TFSA]⁻ isomers were stabilized for enthalpy. $\Delta_{\text{iso}}H(\text{Nd})$ contributed to the remarkable decrease in the $\Delta_{\text{iso}}G(\text{Nd})$ and this result indicated that the *cis*-[TFSA]⁻ bound to Nd³⁺ cation was preferentially stabilized and the coordination state of [Nd^(III)(*cis*-TFSA)₅]²⁻ became steady in [P₂₂₂₅][TFSA].

Furthermore, the optimum geometries and the bonding energies of [RE^(III)(*cis*-TFSA)₄]²⁻ and [RE^(III)(*cis*-TFSA)₅]²⁻ were also determined from DFT simulations

with ADF package. The bonding energy; ΔE_b was estimated from $\Delta E_b = E_{\text{tot}}(\text{cluster}) - E_{\text{tot}}(\text{RE}^{2,3+}) - nE_{\text{tot}}([\text{TFSA}]^-)$. The calculated $\Delta E_b([\text{Nd}^{(III)}(\textit{cis}\text{-TFSA})_4]^{2-})$, $\Delta E_b([\text{Nd}^{(III)}(\textit{cis}\text{-TFSA})_5]^{2-})$, $\Delta E_b([\text{Dy}^{(III)}(\textit{cis}\text{-TFSA})_4]^{2-})$ and $\Delta E_b([\text{Dy}^{(III)}(\textit{cis}\text{-TFSA})_5]^{2-})$ were -2241.6, -4362.3, -2135.4 and -4284.2 kJmol⁻¹, respectively. This result was revealed that [RE^(III)(*cis*-TFSA)₅]²⁻ cluster formed stronger coordination bonds than [RE^(III)(*cis*-TFSA)₄]²⁻ cluster. The average atomic charges and the bond distances of these clusters were consistent with the thermodynamic properties.

ACKNOWLEDGEMENTS

This work was partially supported by the Grant-in-Aid for Scientific Research (No. 15H02848) from the Ministry of Education, Culture, Sports, Science and Technology, Japan.

REFERENCES

- [1] Yang J, Li X, Lang J, *et al.* Synthesis and optical properties of Eu-doped ZnO nano sheets by hydrothermal method. *Mater Sci Semicond Process* 2011; 14: 247-52. <http://dx.doi.org/10.1016/j.mssp.2011.04.002>
- [2] Rao RP, Devine DJ. RE-activated lanthanide phosphate phosphors for PDP applications. *J Lumin* 2000; 87-89: 1260-3. [http://dx.doi.org/10.1016/S0022-2313\(99\)00551-7](http://dx.doi.org/10.1016/S0022-2313(99)00551-7)
- [3] Thiel CW, Böttger T, Cone RL. Rare-earth-doped materials for applications in quantum information storage and signal processing. *J Lumin* 2011; 131: 353-61. <http://dx.doi.org/10.1016/j.jlumin.2010.12.015>
- [4] Yuan D, Liu Y. Electrochemical preparation La-Co magnetic alloy films from dimethylsulfoxide. *Mater Chem Phys* 2006; 96: 79-83. <http://dx.doi.org/10.1016/j.matchemphys.2005.06.052>
- [5] Ono N, Sagawa M, Kasada R, Matsui H, Kimura A. Production of thick high-performance sintered neodymium magnets by grain boundary diffusion treatment with dysprosium-nickel-aluminum alloy. *J Magn Magn Mater* 2011; 323: 297-300. <http://dx.doi.org/10.1016/j.jmmm.2010.09.021>
- [6] Miura K, Itoh M, Machida K. Extraction and recovery characteristics of Fe element from Nd-Fe-B sintered magnet powder scrap by carbonylation. *J Alloys Compd* 2008; 466: 228-32. <http://dx.doi.org/10.1016/j.jallcom.2007.11.013>
- [7] Matsuura Y. Recent development of Nd-Fe-B sintered magnets and their applications. *J Magn Magn Mater* 2006; 303: 344-7. <http://dx.doi.org/10.1016/j.jmmm.2006.01.171>
- [8] Kondo H, Matsumiya M, Tsunashima K, Kodama S. Attempts to the electrodeposition of Nd from ionic liquids at elevated temperatures. *Electrochim Acta* 2012; 66: 313-9. <http://dx.doi.org/10.1016/j.electacta.2012.01.101>
- [9] Kondo H, Matsumiya M, Tsunashima K, Kodama S. Investigation of oxidation state of the electrodeposited neodymium metal related with the water content of phosphonium ionic liquids. *ECS Trans* 2012; 50: 529-38. <http://dx.doi.org/10.1149/05011.0529ecst>
- [10] Tsuda N, Matsumiya M, Tsunashima K, Kodama S. Electrochemical behavior and solvation analysis of rare earth

- complexes in ionic liquids media investigated by SECM and Raman spectroscopy. *ECS Trans* 2012; 50: 539-48.
<http://dx.doi.org/10.1149/05011.0539ecst>
- [11] Ishii M, Matsumiya M, Kawakami S. Development of recycling process for rare earth magnets by electrodeposition using ionic liquids media. *ECS Trans* 2012; 50: 549-60.
<http://dx.doi.org/10.1149/05011.0549ecst>
- [12] Matsumiya M, Ishii M, Kazama R, Kawakami S. Electrochemical analyses of diffusion behaviors and nucleation mechanisms for neodymium complexes in [DEME][TFSA] ionic liquid. *Electrochim Acta* 2014; 146: 371-7.
<http://dx.doi.org/10.1016/j.electacta.2014.09.066>
- [13] Kurachi A, Matsumiya M, Tsunashima K, Kodama S. Electrochemical behavior and electrodeposition of dysprosium in ionic liquids based on phosphonium cations. *J Appl Electrochem* 2012; 42: 961-8.
<http://dx.doi.org/10.1007/s10800-012-0463-8>
- [14] Kazama R, Matsumiya M, Tsuda N, Tsunashima K. Electrochemical analysis of diffusion behavior and nucleation mechanism for Dy(II) and Dy(III) in phosphonium-based ionic liquids. *Electrochim Acta* 113 (2013) 269-279.
<http://dx.doi.org/10.1016/j.electacta.2013.09.082>
- [15] MacFarlane DR, Forsyth M, Howlett PC, *et al.* Ionic liquids in electrochemical devices and processes: managing interfacial electrochemistry. *Acc Chem Res* 2007; 40: 1165-73.
<http://dx.doi.org/10.1021/ar7000952>
- [16] Shamsipur M, Beigi AAM, Teymouri M, Pourmortazavi SM, Irandoust M. Physical and electrochemical properties of ionic liquids 1-ethyl-3-methylimidazolium tetrafluoroborate, 1-butyl-3-methylimidazolium trifluoromethanesulfonate and 1-butyl-1-methylpyrrolidinium bis(trifluoromethylsulfonyl)imide. *J Mol Liq* 2010; 157: 43-50.
<http://dx.doi.org/10.1016/j.molliq.2010.08.005>
- [17] Tsunashima K, Kawabata A, Matsumiya M, *et al.* Low viscous and highly conductive phosphonium ionic liquids based on bis(fluorosulfonyl)amide anion as potential electrolytes. *Electrochem Commun* 2011; 13: 178-81.
<http://dx.doi.org/10.1016/j.elecom.2010.12.007>
- [18] Ohtaki H, Radnai T. Structure and dynamics of hydrated ions. *Chem Rev* 1993; 93: 1157-204.
<http://dx.doi.org/10.1021/cr00019a014>
- [19] Herstedt M, Smirnov M, Johansson P, *et al.* Spectroscopic characterization of the conformational states of the bis(trifluoromethanesulfonyl)imide anion (TFSA). *J Raman Spectrosc* 2005; 36: 762-70.
<http://dx.doi.org/10.1002/jrs.1347>
- [20] Umebayashi Y, Mori S, Fujii K, *et al.* Raman spectroscopic studies and ab initio calculations on conformational isomerism of 1-butyl-3-methylimidazolium bis-(trifluoromethanesulfonyl)amide solvated to a lithium ion in ionic liquids: effects of the second solvation sphere of the lithium ion. *J Phys Chem B* 2010; 114: 6513-21.
<http://dx.doi.org/10.1021/jp100898h>
- [21] Umebayashi Y, Mitsugi T, Fukuda S, *et al.* Lithium ion solvation in room-temperature ionic liquids involving Bis(trifluoromethanesulfonyl) imide anion studied by Raman spectroscopy and DFT calculations. *J Phys Chem B* 2007; 111: 13028-32.
<http://dx.doi.org/10.1021/jp076869m>
- [22] Shirai A, Fujii K, Seki S, Umebayashi Y, Ishiguro S, Ikeda Y. Solvation of lithium ion in N,N-diethyl-N-methyl-N-(2-methoxyethyl)ammonium bis(trifluoromethanesulfonyl)-amide using Raman and multinuclear NMR spectroscopy. *Anal Sci* 2008; 24: 1291-6.
<http://dx.doi.org/10.2116/analsci.24.1291>
- [23] Lassegues J-C, Grondin J, Aupetit C, Johansson P. Spectroscopic identification of the lithium ion transporting species in LiTFSI-doped ionic liquids. *J Phys Chem A* 2009; 113: 305-14.
<http://dx.doi.org/10.1021/jp806124w>
- [24] Fujii K, Nonaka T, Akimoto Y, Umebayashi Y, Ishiguro S. Solvation structures of some transition metal(II) ions in a room-temperature ionic liquid, 1-ethyl-3-methylimidazolium bis(trifluoromethanesulfonyl)amide. *Anal Sci* 2008; 24: 1377-84.
<http://dx.doi.org/10.2116/analsci.24.1377>
- [25] Umebayashi Y, Matsumoto K, Mune Y, Zhang Y, Ishiguro S. Conformational equilibria of solvent N,N-dimethylpropionamide in the bulk and in the coordination sphere of the manganese(II) ion. *Phys Chem Chem Phys* 5 (2003) 2552-2556.
<http://dx.doi.org/10.1039/b302143b>
- [26] Matsumiya M, Kamo Y, Hata K, Tsunashima K. Solvation structure of iron group metal ion in TFSA-based ionic liquids investigated by Raman spectroscopy and DFT calculations. *J Mol Struct* 2013; 1048: 59-63.
<http://dx.doi.org/10.1016/j.molstruc.2013.04.023>
- [27] Matsumiya M. Electrodeposition of rare earth metal in ionic liquids. Application of Ionic Liquids on Rare Earth Green Separation and Utilization (2016) 117-53.
- [28] Furlani M, Ferry A, Franke A, Jacobsson P, Mellander B-E. Time resolved luminescence and vibrational spectroscopic studies on complexes of poly(ethylene oxide) oligomers and Eu(TFSI)₃ salt. *Solid State Ionics* 1998; 113-1155: 129-139.
- [29] Matsumiya M, Kazama R, Tsunashima K. Analysis of coordination states for Dy(II) and Dy(III) complexes in ionic liquids by Raman spectroscopy and DFT calculation. *J Mol Liq* 2016; 215: 308-15.
<http://dx.doi.org/10.1016/j.molliq.2015.12.049>
- [30] te Velde G, Bickelhaupt FM, Baerends EJ, *et al.* Chemistry with ADF. *J Comput Chem* 2001; 22: 931-67.
<http://dx.doi.org/10.1002/jcc.1056>
- [31] Fonseca Guerra C, Snijders JG, te Velde G, Baerends EJ. Towards an order-N DFT method. *Theor Chem Acc* 1998; 99: 391-403.
<http://dx.doi.org/10.1007/s002140050353>
- [32] Baerends EJ, Ros P. Evaluation of the LCAO Hartree—Fock—Slater method: Applications to transition-metal complexes. *Int J Quantum Chem Symp* 1978; 12: 169-90.
- [33] Baerends EJ, Ellis DE, Ros P. Self-consistent molecular Hartree—Fock—Slater calculations I. The computational procedure. *Chem Phys* 1973; 2: 41-51.
[http://dx.doi.org/10.1016/0301-0104\(73\)80059-X](http://dx.doi.org/10.1016/0301-0104(73)80059-X)
- [34] ADF2014.01, SCM, Theoretical Chemistry, VrijeUniversiteit, Amsterdam, The Netherlands.
- [35] Tsunashima K, Sugiyama M. Physical and electrochemical properties of low-viscosity phosphonium ionic liquids as potential electrolytes. *Electrochem Commun* 2007; 9: 2353-8.
<http://dx.doi.org/10.1016/j.elecom.2007.07.003>
- [36] Frisch MJ, Trucks GW, Schlegel HB, *et al.* Gaussian, Inc., Wallingford CT, 2010.
- [37] Harihara PC, Pople JA. Accuracy of AH n equilibrium geometries by single determinant molecular orbital theory. *Mol Phys* 1974; 27: 209-14.
<http://dx.doi.org/10.1080/00268977400100171>
- [38] Ditchfie R, Hehre WJ, Pople JA. Self-consistent molecular-orbital methods. IX. An extended gaussian-type basis for molecular-orbital studies of organic molecules. *J Chem Phys* 1971; 54: 724-8.
<http://dx.doi.org/10.1063/1.1674902>
- [39] Francl MM, Pietro WJ, Hehre WJ, *et al.* Self-consistent molecular orbital methods. XXIII. A polarization-type basis set for second-row elements. *J Chem Phys* 1982; 77: 3654-65.
<http://dx.doi.org/10.1063/1.444267>
- [40] Harihara PC, Pople JA. The influence of polarization functions on molecular orbital hydrogenation energies. *Theor Chim Acta* 1973; 28: 213-22.
<http://dx.doi.org/10.1007/BF00533485>

- [41] Hehre WJ, Ditchfie R, Pople JA. Self-consistent molecular orbital methods. XII. Further extensions of gaussian-type basis sets for use in molecular orbital studies of organic molecules. *J Chem Phys* 1972; 56: 2257-61.
<http://dx.doi.org/10.1063/1.1677527>
- [42] Becke AD. Density - functional thermochemistry. III. The role of exact exchange. *J Chem Phys* 1993; 98: 5648-52.
<http://dx.doi.org/10.1063/1.464913>
- [43] Lee C, Yang W, Parr RG. Development of the Colle-Salvetti correlation-energy formula into a functional of the electron density. *Phys Rev B* 1988; 37: 785-9.
<http://dx.doi.org/10.1103/PhysRevB.37.785>
- [44] Vosko SH, Wilk L, Nusair MC. Accurate spin-dependent electron liquid correlation energies for local spin density calculations: a critical analysis. *Can J Phys* 1980; 58: 1200-11.
<http://dx.doi.org/10.1139/p80-159>
- [45] Perdew JP. Density-functional approximation for the correlation energy of the inhomogeneous electron gas. *Phys Rev B* 1986; 33: 8822-4.
<http://dx.doi.org/10.1103/PhysRevB.33.8822>
- [46] Becke AD. Density-functional exchange-energy approximation with correct asymptotic behavior. *Phys Rev A* 1988; 38: 3098-100.
<http://dx.doi.org/10.1103/PhysRevA.38.3098>
- [47] Slater JC, Johnson KH. Self-Consistent-Field $X\alpha$ Cluster method for polyatomic molecules and solids. *Phys Rev B* 1972; 5: 844-53.
<http://dx.doi.org/10.1103/PhysRevB.5.844>
- [48] van Lenthe E, Baerends EJ, Snijders JG. Relativistic regular two - component Hamiltonians. *J Chem Phys* 1993; 99: 4597-610.
<http://dx.doi.org/10.1063/1.466059>
- [49] Wang SG, Pan DK, Schwarz WHE. Density functional calculations of lanthanide oxides. *J Chem Phys* 1995; 102: 9296-308.
<http://dx.doi.org/10.1063/1.468796>
- [50] Wang SG, Schwarz WHE. Lanthanide diatomics and lanthanide contractions. *J Phys Chem* 1995; 99: 11687-95.
<http://dx.doi.org/10.1021/j100030a011>
- [51] Rey I, Johansson P, Lindgren J, Lassegues JC, Grondin J, Servant L. Spectroscopic and theoretical study of (CF₃SO₂)₂N-(TFSI-) and (CF₃SO₂)₂NH(HTFSI). *J Phys Chem A* 1998; 102: 3249-58.
<http://dx.doi.org/10.1021/jp980375v>
- [52] Castriota M, Caruso T, Agostino RG, Cazzanelli E, Henderson WA, Passerini S. Raman investigation of the ionic liquid N-methyl-N-propylpyrrolidinium bis(trifluoromethanesulfonyl)imide and its mixture with LiN(SO₂CF₃)₂. *J Phys Chem A* 2005; 109: 92-6.
<http://dx.doi.org/10.1021/jp046030w>
- [53] Yaita T, Narita H, Suzuki Sh, Tachimori Sh, Motohashi H, Shiwaku H. Structural study of lanthanides(III) in aqueous nitrate and chloride solutions by EXAFS. *J Radioanal Nucl Chem* 1999; 239: 371-5.
<http://dx.doi.org/10.1007/BF02349514>